Measurements of Ear-Canal Cross-Sectional Areas from Live Human Ears with Implications for Wideband Acoustic Immittance Measurements

Susan E. Voss
Smith College, svoss@smith.edu

Nicholas J. Horton
Amherst College

Katherine E. Fairbank
Smith College

Lu Xia
Smith College

Lauren R. K. Tinglin
Smith College

See next page for additional authors

JASA ARTICLE

Measurements of ear-canal cross-sectional areas from live human ears with implications for wideband acoustic immittance measurements

Susan E. Voss,[1,a)] Nicholas J. Horton,[2,b)] Katherine E. Fairbank,[1] Lu Xia,[1] Lauren R. K. Tinglin,[1] and Kathryn D. Girardin[3]

[1]*Picker Engineering Program, Smith College, Northampton, Massachusetts 01063, USA*

[2]*Department of Mathematics & Statistics, Amherst College, Amherst, Massachusetts 01002, USA*

[3]*Holyoke Medical Center, Holyoke, Massachusetts 01040, USA*

ABSTRACT:

Wideband acoustic immittance (WAI) measures are noninvasive diagnostic measurements that require an estimate of the ear canal's area at the measurement location. Yet, physical measurements of the area at WAI probe locations are lacking. Methods to measure ear-canal areas from silicone molds were developed and applied to 169 subjects, ages 18–75 years. The average areas at the canal's first bend and at 12 mm insertion depth, which are likely WAI probe locations, were 63.4 ± 13.5 and $61.6 \pm 13.5\,\text{mm}^2$, respectively. These areas are substantially larger than those assumed by current FDA-approved WAI measurement devices as well as areas estimated with acoustical methods or measured on cadaver ears. Left and right ears from the same subject had similar areas. Sex, height, and weight were not significant factors in predicting area. Age cohort was a significant predictor of area, with area increasing with decade of life. A subset of areas from the youngest female subjects did not show an effect of race on area (White or Chinese). Areas were also measured as a function of insertion depth of 4.8–13.2 mm from the canal entrance; area was largest closest to the canal entrance and systematically decreased with insertion depth.

 https://doi.org/10.1121/10.0002358

(Received 2 June 2020; revised 7 October 2020; accepted 7 October 2020; published online 24 November 2020)

[Editor: Christopher Shera] Pages: 3042–3051

I. INTRODUCTION

Historically, the ear canal's geometry has been studied in order to facilitate (1) the description of sound transmission from the outer ear to the middle ear, (2) a description of the sound field as a function of position along the ear canal, and (3) methods to calculate the sound field at the tympanic membrane based on a microphone measurement within the ear canal (Egolf *et al.*, 1993; Stinson and Lawton, 1989). Additionally, the cross-sectional area of the ear canal is required for some clinical applications, such as wideband acoustic immittance (WAI) measurements that have been extensively discussed in the literature and have been applied to a range of clinically-relevant diagnostic issues (e.g., Feeney, 2013). As an example, the WAI quantity of pressure reflectance is typically calculated from an impedance measurement in the ear canal $Z_{EC}(f)$ and an estimate of the corresponding cross-sectional area of the canal A as

$$R(f) = \frac{Z_{EC}(f) - \frac{\rho c}{A}}{Z_{EC}(f) + \frac{\rho c}{A}}, \quad (1)$$

where ρ and c are the density of air and the speed of sound in air, respectively. The common WAI quantities of power (or energy) reflectance and absorbance are calculated directly from Eq. (1) and are thus dependent on the canal's area. Similarly, an accurate determination of ear-canal area is also needed for some methods of *in situ* sound calibration (Souza *et al.*, 2014).

Nonetheless, while the description of the ear canal's geometry is essential for a range of scientific and clinical applications, there are relatively few data that directly describe its anatomy, and these limited data suggest substantial variations in ear-canal anatomy among individuals. The typical textbook description of the ear canal is not detailed and is fairly consistent across authors and decades. As an example, Møller (2006) reads:

"The ear canal has a length of approximately 2.5 cm and a diameter of approximately 0.6 cm. It has the shape of a lazy S. The most medial part is a nearly circular opening in the skull bone, and the outer part is cartilage. The outer cartilaginous portion of the ear canal is also nearly circular in young individuals but with age the cartilaginous part often changes shape and attains an oval shape."

Other books offer similar descriptions, and yet specific references to publications that report measurements of the length and diameter of the ear canal are not provided, nor are publications that describe changes with age (e.g., Donaldson *et al.*, 1992; Wever and Lawrence, 1954; Zemlin, 1988).

The most detailed scientific descriptions of the ear canal's geometry, and more specifically its cross-sectional

a)Electronic mail: svoss@smith.edu
b)ORCID: 0000-0003-3332-4311.

area, come from three sources: A letter to the editor of Acustica from Johansen (1975) and published studies from Stinson and Lawton (1989) and Egolf *et al*. (1993). All three of these studies used cadaveric ear canals and reference ear-canal locations as the distance from the tympanic membrane. In contrast, the work presented here uses live human ears and the entrance of the ear canal as a reference location because the canal entrance is the physical reference available when making ear-canal based measurements on live human subjects, as with WAI measurements.

The majority of published WAI measurements come from ear-canal probes that are identical or similar to the probes on either the Mimosa Acoustics HearID system or the Interacoustics Titan system (Voss, 2019), which are capable of insertion depths from the concha of about 12 mm or less. To date, there is inadequate detail on the variation of the ear-canal cross-sectional area at these insertion depths, which are closer to the canal entrance than to the tympanic membrane. The aforementioned publications will be further detailed in Sec. IV so that they can be compared to the work presented here.

Shahnaz and Bork (2006) reported significant differences in wideband reflectance between normal-hearing White and Chinese young adults, but reasons for the differences are not yet known. One possibility is differences in ear-canal cross-sectional area between these racial groups.

The goal of this work is to describe the size and variability of ear-canal areas at positions that correspond to the insertion depths for probes used to make WAI measurements. In particular, areas from silicone molds of adult ear canals are measured and analyzed to answer these five questions:

(1) How does ear-canal area vary across adult ears at a typical measurement probe's location?
(2) Are left and right ear-canal areas from the same subject similar?
(3) How is ear-canal area associated with age, sex, height, or weight?
(4) How does ear-canal area change with distance from the canal entrance?
(5) Are their systematic differences in ear-canal areas between young White and Chinese female subjects?

II. METHODS

A. Subjects

Measurements were approved by the Smith College Institutional Review Board, and each subject provided written consent. Once consented, each subject filled out an intake form and self-reported their age, sex, weight, height, and race; for the results presented here, "Chinese" is defined as Asian with four grandparents all born in China. Next, each subject underwent an exam by a licensed audiologist (K.G.) that included (1) otoscopic inspection of their ear canal for excessive wax that might be pushed toward the tympanic membrane and potentially lead to impaction, (2) a 226 Hz tympanogram, and (3) an air-bone gap audiogram. Ears were excluded if they had excessive wax or abnormal tympanograms or abnormal air-bone gaps (i.e., greater than 20 dB at any of the frequencies 500, 1000, 2000, and 4000 Hz). Silicone molds were made by audiologist K.G. on all remaining ears.

Figure 1 summarizes the subject demographics for the $N = 169$ subjects on whom silicone molds were made; in most cases, molds were made on both the right and left ear, but not in all cases (due to unilateral wax or middle-ear abnormality). The initial recruitment goal was for ten female and ten male subjects in each decade of adult life from 18 to 80 years of age; subjects were binned into age cohorts defined by decade of life. Additional female subjects in the 18–29 year old age cohort were recruited, with an initial goal motivated by the work of Shahnaz and Bork (2006) to determine if racial differences exist in ear-canal areas; females in the age group of 18–29 were selected because of the potential subject pool at Smith College, which is an all-women's college with a substantial international student population. As detailed below, a majority of the ear-canal molds from the young female subject cohort were used to develop area-measurement techniques, and some of these molds were damaged and only partially available for their initial purpose.

B. Ear-canal molds

All silicone ear molds were made by the same audiologist (author K.G.). These were closed jaw impressions with no bite block, no gum chewing, and no talking. A foam otoblock with removal string was placed into the ear canal and silicone impression material (Westone SiliClone 48ML) was injected into the ear canal with a manual impression gun (for DM-50 ML cartridges). The Westone SiliClone 48ML is a soft vinyl polysiloxane material and was chosen for its low viscosity which minimizes distortion and pressure on the ear-canal wall (Pirzanski and Berge, 2002). When injected, the soft malleable material entered the canal and cured to the shape of the canal in 4–7 min; a fingernail was used to gently touch the mold to make sure it was set before removing it from the canal. A typical set of molds from one subject is photographed in Fig. 2. Molds were stored in individual plastic bags in a climate-controlled lab, and digital scans of them were made 4–12 months after the molds were made.

C. Digitization of the molds

The molds were scanned (digitized) with a *3Shape H600* Desktop Scanner. First, the otoblock was removed from each pair of ear impressions. Next, magnetic pins were inserted in each mold and placed on the corresponding magnetic receptacles inside the three-dimensional (3D) scanner. Next, the scanner's companion software *3ShapeAudio* scanned and saved the subject's left and right ear molds. The resulting scans were automatically saved in *.stl* format.

Age Range (Years)	Sex	Number Subjects	1st Bend Measurements			12mm Measurements		
			Both Ears	Left Only	Right Only	Both Ears	Left Only	Right Only
18-29	F	41	40	0	1	6	0	0
18-29	M	11	11	0	0	11	0	0
30-39	F	14	11	2	1	11	2	1
30-39	M	11	10	1	0	10	1	0
40-49	F	10	10	0	0	10	0	0
40-49	M	9	9	0	0	9	0	0
50-59	F	11	11	0	0	11	0	0
50-59	M	12	11	0	1	11	0	1
60-69	F	14	12	1	1	12	1	1
60-69	M	12	9	2	1	9	2	1
70-79	F	11	10	0	1	10	0	1
70-79	M	13	12	1	0	12	1	0
TOTAL		**169**	**156**	**7**	**6**	**122**	**7**	**5**

FIG. 1. Subject demographics for which silicone molds were made in left and right ear canals. "1st Bend Measurements" refers to the ability to identify and measure the cross-sectional area at the first bend, and "12 mm Measurements" refers to the ability to measure a cross-sectional area at a distance 12 mm from the ear-canal entrance. Note, the silicone molds from the first 35 subjects recruited in the 18–29 years cohort were used to develop area-measurement methods and were manipulated in a way that prevented identification of a 12 mm insertion location.

Ultimately, areas were measured from the .stl files with ShapeDesigner software (3ShapeAudio).

D. Definition of the ear-canal entrance and measurement of area

This work is motivated by the need to determine the cross-sectional area at a typical location of a WAI measurement probe within the canal. As a starting point, we measured the ear-canal area at a 12 mm insertion depth from the entrance of the canal. This location was chosen because the Etymotic Research system's ER10c transducer coupled to their 14 A yellow foam eartip is a common probe for WAI measurements, and this foam tip is 12 mm long. Additionally, previous work has controlled for the probe position to be such that the yellow foam tip sits at a position judged to have the lateral edge of the foam tip flush with the entrance to the ear canal, resulting in this 12 mm insertion depth (e.g., Abur *et al.*, 2014). The method used to define the ear-canal entrance and determine a 12 mm insertion on the digitized silicone molds is described in Fig. 3. Once ear-canal measurements were made at the 12 mm insertion depth, additional area measurements were made in 0.6 mm increments that ranged from insertion depths of 4.8 to 13.2 mm from the canal entrance. At each location, the ear-canal area was measured as the area of a cross-sectional slice normal to the canal axis. On some molds at some locations greater than 12 mm, the molds were not fully formed and area measurements were not able to be made.

FIG. 2. (Color online) The left and right impressions from one subject.

E. Area at the first bend of the ear canal

The first bend of the ear canal was identified, and both (1) the area was measured at the location of the first bend

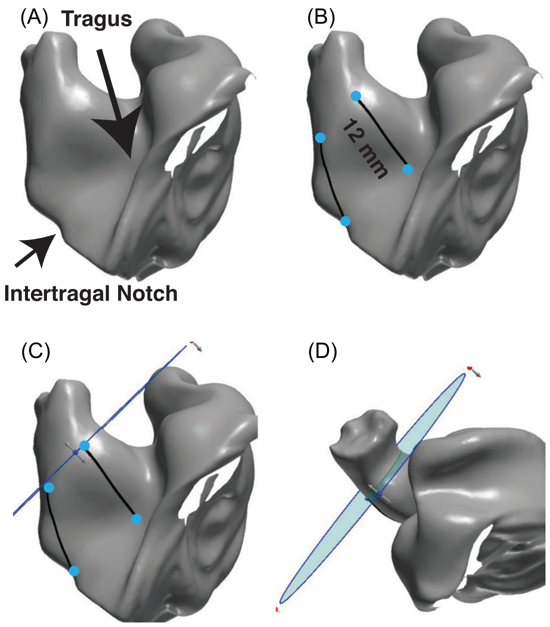

FIG. 3. (Color online) Scanned and labeled left ear-canal mold showing the process used to define each ear-canal entrance and measure each area. (A) An indentation from the tragus was visible on each mold as a roughly fan-shaped indentation in the anterior canal wall where the canal and concha meet. The deepest part of this indentation is used to define the "tragus" measurement location; it can be difficult to see the indentation on a two-dimensional (2D) image, but it is possible to identify it when the scanned model is rotated on the computer screen and simultaneously compared with the physical mold. The intertragal notch is at the inferior surface or floor of the ear canal where the tragus meets the antitragus. (B) Using ShapeDesigner software, the tragus and intertragal notch were marked with dots, and lines of length 12 mm were drawn and marked along the surface into the canal with the software. After these lines were marked, the yellow foam plug was held along the physical ear-canal mold and visually compared to the location on the digital mold to ensure consistency in the location estimate. (C) A plane was drawn that included the two 12 mm measurements, and the plane was manipulated to be normal to the axis of the ear canal. This manipulation included slight rotations and translations from the 12 mm estimate so that the plane appeared visually normal (orthogonal) to the central axis of the ear canal. (D) A rotated view of the plane drawn in (C) so that the plane can be seen to be normal to the axis of the ear canal. Once this plane was set, the area was measured and reported with the ShapeDesigner software.

and (2) the distance between the first bend and the 12 mm insertion depth location was measured; this latter measurement was used to calculate the distance from the canal entrance to the first bend. The area at the first bend is relevant to our work for several reasons. First, the first bend is easily identifiable in most ear-canal molds, although there is substantial variability in the extent of the bend. In some ears, the bend appears to be substantial enough that it would be difficult to pass a probe such as the Etymotic Research system's ER10c transducer past the first bend; thus, in some ears this bend can act as an effective marker of a possible measurement location. Second, as described below, we were able to make an area measurement for all of our molds at the first bend but not all of them at 12 mm insertion due to the lack of a tragus imprint on some molds; thus, measurements at the first bend provide a larger data set within our specimens. This larger dataset is relevant because one of the findings of this work is that the first bend and the 12 mm insertion depth are at similar locations (see Sec. III).

F. Methods development and partial mold loss from youngest female cohort

The silicone molds from the first 35 subjects recruited in the 18–29 year cohort were used to develop methods; they were scanned initially by a 3D-scanner that was not designed for ear molds and required the molds to be cut to shorter specimens to fit in the scanner. Unfortunately, the manipulations made to the molds to fit them in the scanner made it impossible to measure the insertion depth relative to the entrance of the ear canal because the anatomical tragus and antitragus markers (Fig. 3) were no longer part of the mold. We were, however, able to identify the first bend and measure its corresponding area on these manipulated molds.

G. Repeated measurements and consistency check

Three independent sets of measurements were made of the areas from each ear mold by different researchers. First, as part of her Smith College undergraduate thesis, Xia (2017) measured the area at the first bend and at the 12 mm insertion, as defined by a single 12 mm measurement from the tragus (did not include the measurement from the antitragus). Later, author Voss repeated these measurements at both the first bend and at the 12 mm insertion depth using the methods described in Fig. 3 to define the insertion location. After these measurements were made, authors Fairbank and Tinglin repeated the measurements using the methods described in Fig. 3 and extended the work to include measurements at 0.6 mm increments along the length of the canal.

Correlation coefficients show the measurements from these three independent sets of measurements are consistent with each other. Specifically, for the measurements at the 12 mm insertion depth, the correlation coefficient between Xia and Fairbank measurements is 0.94, the correlation coefficient between Voss and Fairbank measurements is 0.93, and the correlation coefficient between Xia and Voss is 0.95. These correlations demonstrate that the methods applied to measure the ear-canal mold areas are repeatable, even with different investigators applying them. The measurements presented in this publication are those measured by Fairbank and Tinglin, as this data set also includes additional areas measured in 0.6 increments along the length of the mold.

H. Statistical analysis

All analyses were undertaken using R (R Core Team, 2020) version 4.0.0. Comparisons of ear-canal area measurements at the first bend and at 12 mm insertion use a generalized estimating equation (Horton and Lipsitz, 1999; Zeger and Liang, 1986) approach with independence working correlation and empirical variance to account for the repeated measurements of ear canal from both the left and right ears of most subjects. Later analyses used the average

https://doi.org/10.1121/10.0002358

of the left and right measurements to yield one observation per subject (91% of subjects had measurements on both left and right ears; for the remainder, the observed value was used). Correlation coefficients were used to calculate the linear associations between two quantitative measurements while a paired t-test was used to compare results between left and right ears.

A multiple linear regression model including main effects was used to assess the associations between ear area and age cohort, sex, weight, and height. Non-significant predictors were dropped from the model. No adjustment for multiple comparisons was undertaken.

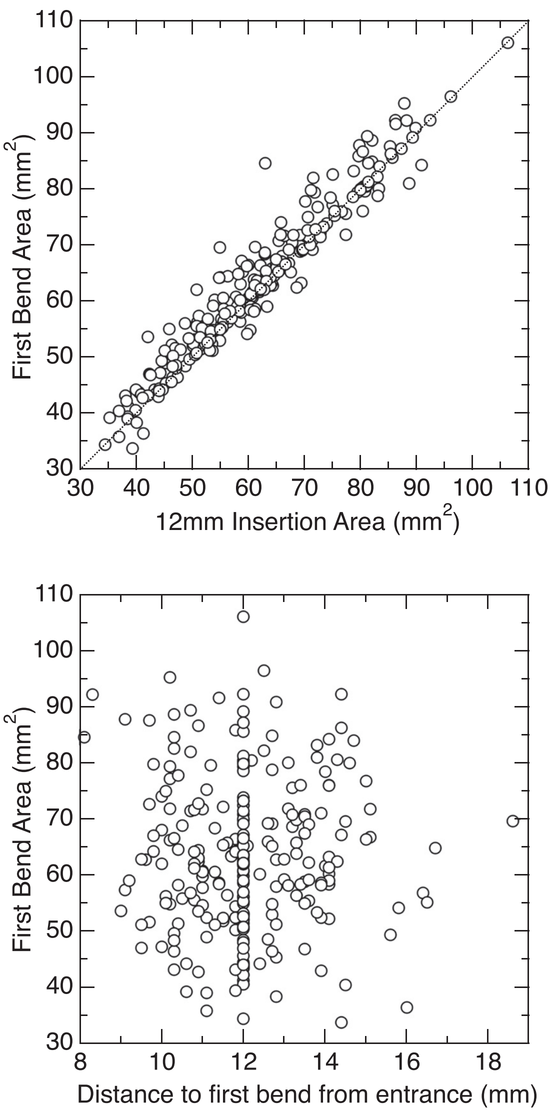

FIG. 4. Upper: Measurements of ear-canal cross-sectional areas at the first-bend location versus the areas measured on the same canals at the 12 mm insertion location ($N = 256$); by definition, the two areas are identical when the first bend occurs at an insertion depth of 12 mm. The correlation between the area measured at the first bend and the 12 mm insertion depth is r = 0.96 ($p < 0.0001$). A test that the difference between the first bend measure and the 12 mm location is zero yielded a 95% confidence interval for the true difference that ranges from 1.3 to 2.2 mm^2 (p-value <0.0001). Lower: Measurements of the ear-canal area at the first bend versus the distance from the ear-canal entrance to the first bend.

III. RESULTS

A. Ear-canal area measurements at first bend and at 12 mm insertion locations

Figure 4 (upper) plots data from all ears (both left and right) where measurements exist for both locations of the first bend and 12 mm insertion locations ($N = 256$). This scatter plot compares the ear-canal area at the first bend of the ear canal to the area at an insertion depth of 12 mm from the ear-canal entrance. Across all ears, the area at either location ranges from 34 to 106 mm^2. The mean $\pm$ standard deviation (SD) is 63.4 $\pm$ 13.5 and 61.6 $\pm$ 13.5 mm^2, respectively, at the first bend and 12 mm locations. The observed difference in area between these two measurement locations is 2.5% of the total area range.

Figure 4 (lower) shows the area at the first bend as a function of the distance to the first bend from the canal entrance. Eighty-one percent of the ears have a first bend that is a distance of 12 $\pm$ 2 mm from the canal entrance, and there is little evidence that the distance to the first bend is associated with the area at the first bend. Additionally, there is little evidence for an association between age and distance to the first bend (not plotted).

B. Left versus right ears

Figure 5 is a scatter plot of ear-canal areas for the left versus right ear of a given subject; areas for both the first bend and the 12 mm insertion depth are displayed, and the assumed areas from the two FDA approved devices (HearID and Titan)

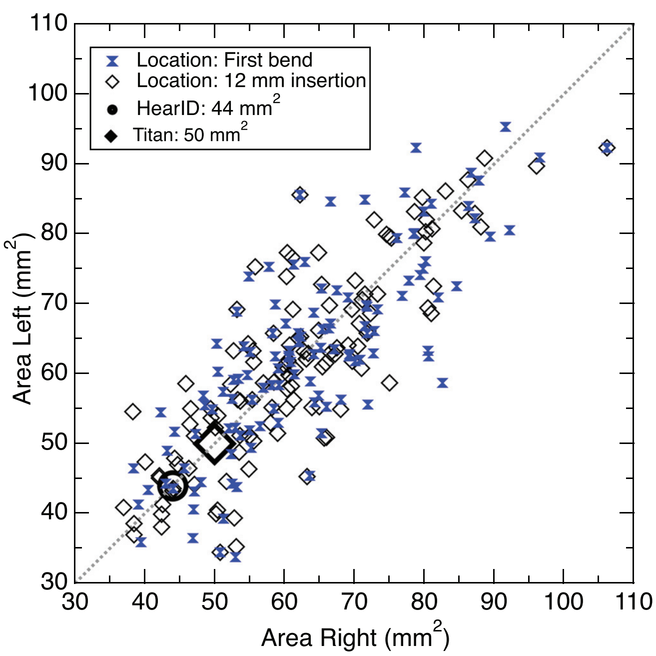

FIG. 5. (Color online) Left versus right ear-canal areas at two locations from subjects on which bilateral molds and measurements were made: 12 mm insertion (black diamond) and first bend (blue hourglass). The dotted line indicates left area = right area. The areas assumed by the HearID and Titan instruments are 44 mm^2 (center of open circle) and 50 mm^2 (center of open diamond), respectively.

https://doi.org/10.1121/10.0002358

are indicated on the plot. At each location, a paired t-test found little evidence for differences between left and right areas. The 95% confidence interval for the mean difference in area between the left and right ear at the first bend was −1.5 to +1.1 mm^2 ($p = 0.77$) and between the left and right ear at 12 mm was −1.8 to +1.0 mm^2 ($p = 0.62$).

C. Potential predictors of area: Age, sex, height, or weight

A multiple regression model was used to simultaneously account for age cohort, sex, height, and weight as potential predictors of ear-canal area. For subjects with measurements from both their left and right ears, the average area was used, as these areas do not show systematic left-right differences (Sec. III B), and when an area measurement existed for only the left or the right ear, then that single measurement was used.

At both locations (first bend and 12 mm insertion), sex, height, and weight were not significant factors and were dropped from the model: sex (first bend $p = 0.20$; 12 mm $p = 0.61$), height (first bend $p = 0.44$; 12 mm $p = 0.93$), and weight (first bend $p = 0.25$; 12 mm $p = 0.19$).

In contrast, age cohort was a significant predictor of area at both locations: first bend ($df = 5$, $p < 0.0001$) and 12 mm insertion ($df = 5$, $p = 0.009$). Figure 6 illustrates the cross-sectional area at the first bend (left) and at 12 mm insertion (right) for age cohorts grouped by decade of life.

D. Area as a function of distance from the canal entrance

Area measurements were made in 0.6 mm increments at insertion depths that ranged from 4.8 to 13.2 mm. Figure 7 plots these areas as a function of insertion depth with age cohort and sex as parameters. In general, the canal area decreases with insertion depth, and the decrease slows down with increasing insertion depth, suggesting a more constant area as the first bend is approached. Additionally, the areas trend upward with increasing age cohorts.

E. Comparison of areas from young White and Chinese female subjects

Ear-canal areas were compared within a subset of younger female subjects (age less than 25 years) between Chinese [$n = 13$, mean = 46.4 mm^2, SD = 13.0 mm^2] and

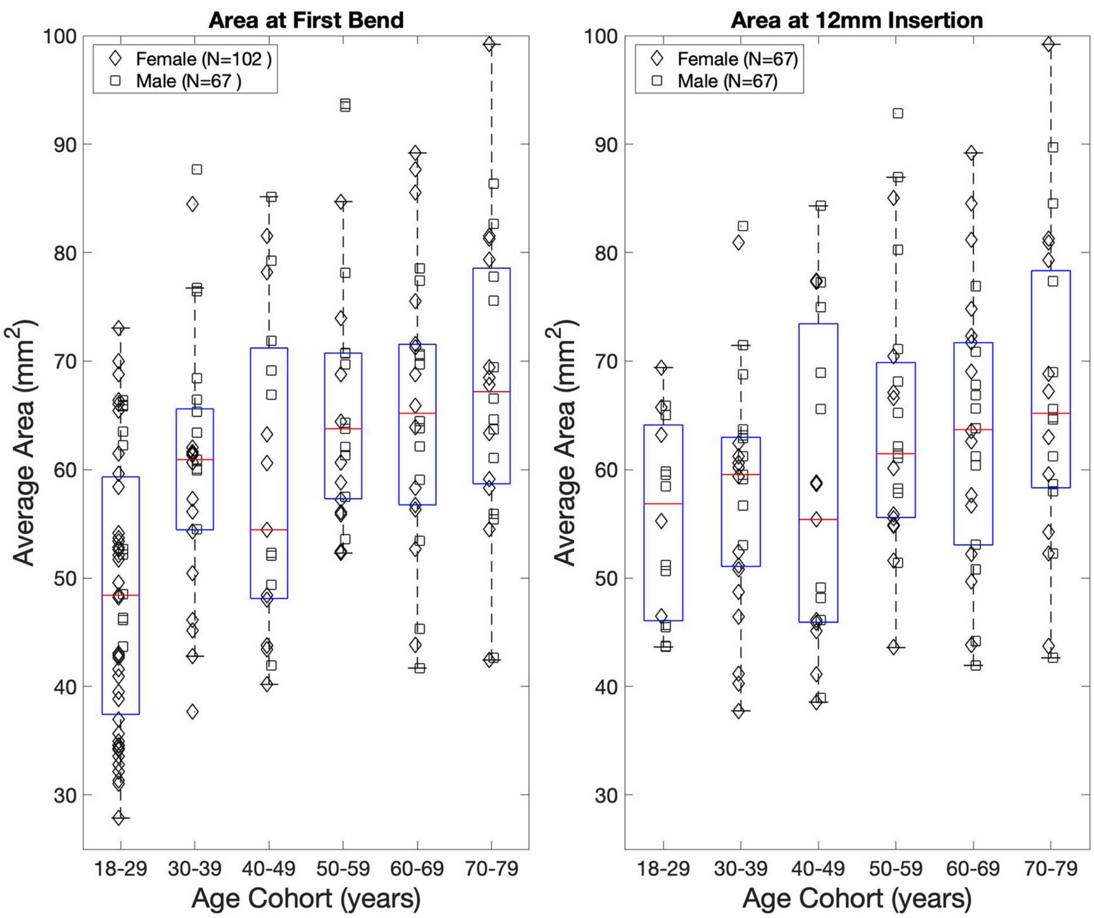

FIG. 6. (Color online) Cross-sectional area at the first bend (left) and 12 mm insertion (right) depths for age cohorts grouped by decade of life. The average of the left and right ear were used for the subjects with bilateral area measurements (Fig. 1), and the individual right or left area measurement was used for the remaining subjects. Each box and whisker plot indicates the age group's median value with the red line and the edges of each box are the 25th and 75th percentiles. Individual area measurements are indicated by diamonds (female) and squares (male). Females have more data in the 18–29 years cohort at the first bend than at 12 mm insertion because area measurements as a function of insertion depth were not available for 35 of these subjects (Sec. II).

https://doi.org/10.1121/10.0002358

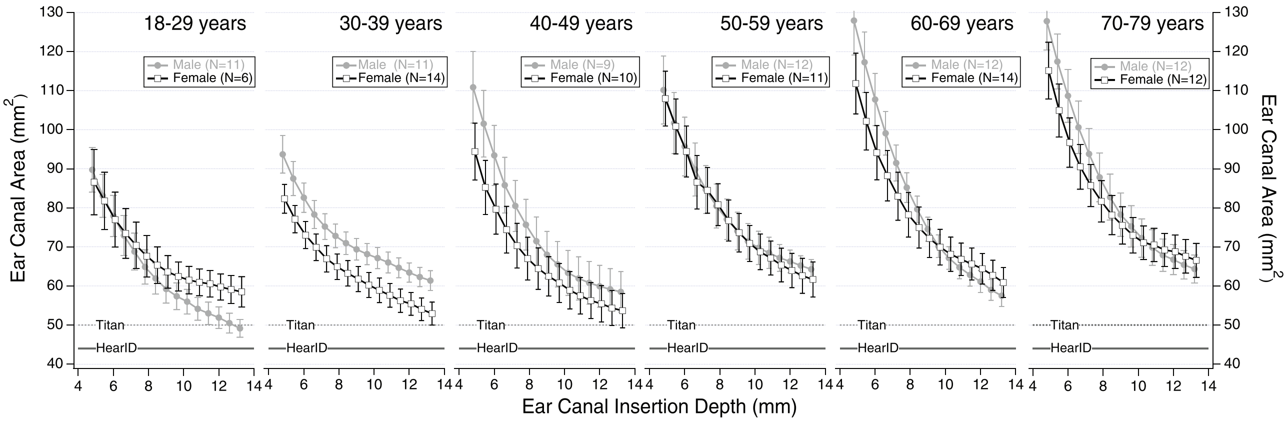

FIG. 7. Mean cross-sectional area as a function of depth into the ear canal relative to the canal entrance for each age cohort, stratified by sex. The average of the left and right ear was used for the 122 subjects with bilateral area measurements (Fig. 1), and the individual right or left area measurements were used for the remaining 12 subjects. The error bars indicate standard errors. The average areas for all ages and all locations are generally larger than the areas assumed by the two commercial WAI instruments, HearID, and Titan, with the indicated assumed areas of 44 and 50 mm^2, respectively.

White ($n = 16$, mean $= 49.8\,\text{mm}^2$, SD $= 12.8\,\text{mm}^2$) subjects. A two-sample unequal variance t-test yielded a p-value of 0.49, and the 95% confidence interval for the difference between Caucasian and Chinese ear areas ranged from 13.3 to $-6.6\,\text{mm}^2$.

IV. DISCUSSION

A. There is substantial variation in ear-canal areas across adult ears at a measurement probe's location

Ear-canal area measurements were analyzed in detail at two locations: (1) the first-bend of the canal and (2) at a 12 mm insertion depth. The ear-canal areas were similar at these two locations, and showed substantial intersubject variation, ranging from about 35 to about 105 mm^2 (Fig. 4).

This finding is clinically relevant because the computation of some WAI quantities (e.g., reflectance, absorbance) depends on the area of the ear canal at the probe location. The assumed ear-canal areas for the two FDA-approved devices are substantially smaller than the mean areas determined in this work. Analyses of WAI measurements made on the same set of ears for which areas are presented here demonstrate that significant differences exist in reflectance when the actual ear-canal area is used instead of the device-assumed area (Balouch *et al.*, 2020; Xia, 2017). Thus, the continued development of WAI measurements for clinical diagnoses will benefit from better descriptions of the ear-canal's area.

B. Left and right areas from the same subject are similar

There was little evidence for differences in area between a subject's left and right ears at both the first-bend location and at the 12 mm insertion. At both locations, the 95% confidence interval for the differences between the left and right ear's areas included zero and were within 2 mm^2 of zero. Thus, if the area of only a subject's left or right ear is known, that area can be assumed to be a reasonable estimate for the area of the other ear.

C. Ear-canal area is associated with age and not associated with sex, height, or weight

At both the first bend and 12 mm insertion depth, there is no indication that the ear-canal area depends on sex, height, or weight of a subject. In contrast, there is evidence that ear-canal area increases with increasing age cohort (Fig. 6); this result suggests that when individual measurements of ear-canal area are not available, calculations of WAI measures might best employ average areas that depend on the age of the subject.

D. How does ear-canal area change with distance from the canal entrance?

Figure 7 demonstrates that there are large variations in ear-canal area both (1) within an individual canal in the range of the canal entrance to several mm insertion into the canal and (2) across subjects binned into age cohorts. In particular, the current assumptions made by the only two FDA approved WAI measurement systems of a single average adult ear-canal area of 44 mm^2 (HearID) and 50 mm^2 (Titan) are both substantially lower than any of the mean areas measured in this work. Additionally, while the HearID probe may sit 12 mm from the canal entrance, it is likely that the Titan probe sits closer to the entrance because the Titan probe is a few mm shorter than the HearID probe; the probe geometry likely results in a larger canal area for the Titan probe than the areas at a 12 mm insertion. Thus, WAI measurements from these two different systems, made on the same ears, likely have different corresponding canal areas due to different probe locations in the ear canal.

E. There is not strong evidence for systematic differences in ear-canal area between younger White and Chinese female subjects

We were motivated to investigate ear-canal area differences between White and Chinese subjects because Shahnaz and Bork (2006) found differences in reflectance between these two groups. Our subject availability was strongest for females in their early 20s and we were able to recruit 13 Chinese and 16 White female subjects less than 25 years of age. While this is a relatively small subject pool, the analysis does not show strong differences in area between the two groups; the White subjects have an average area that is 3.4 mm^2 larger than the Chinese subjects, but the confidence interval is large and the difference is not significant. While our comparison has limited power due to small sample size, the results suggest that the differences reported by Shahnaz and Bork (2006) may not be solely due to differences in ear-canal areas.

F. Comparison to published area measurements

We have identified four publications that report physically-measured ear-canal areas (Egolf *et al.*, 1993; Johansen, 1975; Stinson and Lawton, 1989; Voss *et al.*, 2008), and there are two major differences between these publications and the work here. First, the published areas are all from *cadaver* ears, whereas the work here is from silicone molds of *live* ears. Second, the published work references ear-canal area locations relative to the tympanic membrane, whereas the work here references the area locations to the entrance of the ear canal, which is needed for live ears for which the location of the tympanic membrane is not available.

Figure 8 compares the area measurements from this work to the published areas from cadaver ear canals. The gray shaded region summarizes areas from Fig. 7, collapsed across age and sex. The ear-canal entrance was mapped to 35 mm distance from the tympanic membrane in order to facilitate the comparison, as the distance from the tympanic membrane is unavailable in the live ears, and canal length is not constant across all ears. We acknowledge that while this choice of 35 mm is somewhat arbitrary, it is based on the following considerations. First, Stinson and Lawton (1989) report canal lengths that range from 27 to 35 mm, and their methods of defining the entrance to the ear canal appear to likely choose a more medial location than the methods presented here. Specifically, Stinson and Lawton (1989) define the canal entrance as the location where the transition between the canal and concha occurs as an estimate of "where the cross-sectional area of the canal increases more rapidly and from visual inspection of the original molds." Our definition of canal entrance (Fig. 3), is lateral to where the cross-sectional area of the canal increases rapidly. Thus, our choice of 35 mm matches the longest canal measured by Stinson and Lawton (1989). A second argument for the choice of mapping the data presented in this work to a 35 mm canal length is that impedance measurements made in these same ears Balouch *et al.* (2020) have quarter-wavelength resonances consistent with an average canal length of 35 mm if one assumes a cylindrical canal and rigid termination and adds 12 mm to account for the probe tip.

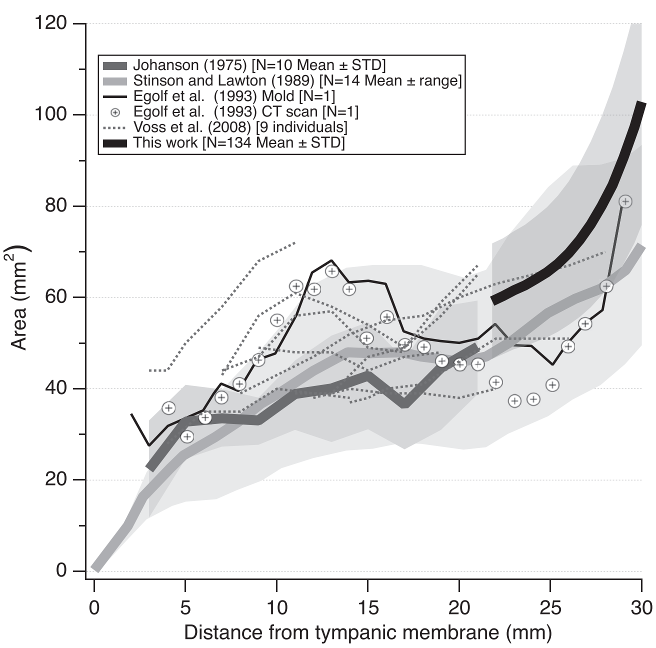

FIG. 8. (Color online) Comparisons of the area measurements in this work to published physical area measurements cadaver ear canals. The gray shaded region summarizes areas from Fig. 7, collapsed across age and sex. The ear-canal entrance from this work was mapped to assume an ear-canal length of 35 mm, as justified within the Sec. IV; however, this is an assumption because ear-canal length is unknown for the live ears. Note, measurements were made from 4.8 to 13.2 mm medial to the ear-canal entrance; thus, the plotted measurements range from distances of from 21.8 to 30.2 mm.

The areas measured for this work in the live ears are larger than those reported in the literature from cadaver ears. It is possible that there are physiological changes between life and death that could result in different areas, such as increased fluid retention along the surface of the ear canal if the cadaver material was stored in fluid. Additionally, the cadaver studies had different methods, which are summarized here in chronological order.

Johansen (1975) used silicone molds from ten human cadaver ear canals and measured canal volume via immersion in 60% alcohol liquid. Canal lengths (mean $\pm$ 1 SD) were reported as 25.7 ± 1.9 mm. No definition for the entrance to the canal was given and a method for measuring the canal length was not given.

Stinson and Lawton (1989) made silicone molds on 15 human cadaver ear canals and used measurements from these molds to describe the geometry of the entire ear canal. They found substantial variability in the anatomy; in particular, in the middle portion of the ear canals, the cross-sectional areas ranged from 25 to 70 mm^2. Across the 15 ear canals, they estimated ear-canal lengths that range from 27 to 35 mm.

Egolf *et al.* (1993) published ear-canal area measurements from a single cadaver ear that were obtained from both computed tomography (CT) scans and from a silicone mold, and they demonstrated the two methods provided similar but not identical estimates of area. They identified the entrance to the canal as the "concha canal interface," but this entrance location was not clearly defined; their measured canal length was 30 mm, and their Fig. 6 would be consistent with a canal length on the order of 30–35 mm with our definition of canal entrance.

Voss *et al.* (2008) measured ear-canal areas from silicone molds taken on nine cadaver ears, and they performed acoustic measurements to assess the accuracy of the acoustically-calculated area method from Keefe *et al.* (1993), which used the real part of the impedance to estimate canal area. Percent differences between the mold and acoustic areas ranged from −54% to 306% with a mean difference of 38%.

Since Voss *et al.* (2008) was published, additional acoustical methods have been suggested to calculate ear-canal areas from impedance measurements, including estimating the surge impedance (Rasetshwane and Neely, 2011), improved methods to utilize the real part of the impedance (Keefe *et al.*, 2015), and minimizing the non-causality in the frequency-domain reflectance via the Hilbert transform and compensating for the effects of evanescent modes (Nørgaard *et al.*, 2017). These acoustical methods all differ in substantial ways, and each has important sets of assumptions that need further validation. Moving forward it will be important to compare acoustically measured areas to physically measured areas in the same ears in order to understand how well the two correspond; we encourage physical ear-canal area measurements to be made in conjunction with measurements that acoustically estimate area so that the relationship between physical area and acoustic estimates of area can be better understood.

G. Subjective aspects of methods and future work

There are subjective aspects to the measurement protocol employed here. First, there is no definitive definition for the entrance to the ear canal, and here it was defined by two points that could be identified on each mold (Fig. 3). Second, the location that a 12-mm-long eartip sits into the ear canal was used to develop methods for defining the insertion depth; in this way, the Etymotic Research 14 A yellow foam tip was held along the edge of each ear mold and it was visually confirmed that measurements of 12 mm along the edges of the ear canal led to a location consistent with the digital measurement of 12 mm described in the methods. Once this 12 mm insertion depth was estimated, the adjustment of the cross-sectional area plane to be orthogonal to the central axis of the ear canal was made visually and was thus also subjective.

Given these subjective aspects of the measurements, at least two lines of argument support that the measurements are representative of the cross-sectional areas at the reported locations. First, changes in area along the canal are relatively small near the 12 mm insertion depth (Fig. 7), so errors on the order of a few mm in estimating the 12 mm insertion depth would likely have effects of less than 10% on the reported area; the percent change in the average area between the 12 and 10.8 mm insertions is 3.9% and between the 12 and 13.2 mm insertions it is −3.9%. Second, once the 12 mm insertion depth was identified, the ability to visually create a plane orthogonal to the central axis was tested by both:

(1) Making multiple area measurements with the plane tilted in different orientations and demonstrating small (on the order of a few mm^2) changes in the measured areas, and
(2) Three independent sets (by different investigators) of area measurements made on all ears gave similar results, as detailed in the Sec. II.

Future work is needed to determine how to define the entrance of the ear canal, the resulting length of the canal, and the location that the tip of an earprobe sits in the canal. Additionally, improvements can be made in defining both the central axis of the ear canal and the plane that is orthogonal (normal) to that axis. Stinson and Lawton (1989) used a mechanical system to measure the 3D ear-canal geometry from the surfaces of ear molds from cadavers, and these measurements were used to calculate a mathematical description for the central axis of the canal and corresponding cross-sectional areas. While such calculations are beyond the scope of this work, future work could also utilize digitized molds and finite-element-modeling software to better define the geometry of the ear canal.

ACKNOWLEDGMENTS

This work was funded by Grant No. R15 DC014129 from the National Institutes of Health NIDCD. We thank Jingping Nie and Tinli Yarrington for their help in organizing some of the silicone ear-canal molds.

Abur, D., Horton, N. J., and Voss, S. E. (**2014**). "Instrasubject variability in power reflectance," J. Am. Acad. Audiol. **25**, 441–448.
Balouch, A. P., Rosenstein, S., Horton, N. J., and Voss, S. E. (**2020**). "Titan and HearID WAI measurements in the same human ears," in *Abstracts from the 47th Annual Scientific and Technology Conference of the American Auditory Society* (American Auditory Society, Scottsdale, AZ), Poster #10, available at https://www.amauditorysoc.org/past-conferences.
Donaldson, J. A., Duckert, L. G., Lambert, P. M., and Rubel, E. W. (**1992**). *Anson Donaldson Surgical Anatomy of the Temporal Bone*, 4th ed. (Raven Press, New York).
Egolf, D. P., Nelson, D. K., Howell, H. C., and Larson, V. D. (**1993**). "Quantifying ear-canal geometry with multiple computer-assisted toographic scans," J. Acoust. Soc. Am. **93**(5), 2809–2819.
Feeney, M. P. (**2013**). "Eriksholm Workshop: Wideband Absorbance Measures of the Middle Ear," Ear Hear. **34**, 78S–79S.
Horton, N. J., and Lipsitz, S. R. (**1999**). "Review of software to fit generalized estimating equation (GEE) regression models," Am. Stat. **53**, 160–169.
Johansen, P. A. (**1975**). "Letters to the editor: Measurement of the human ear canal," Acustica **33**, 349–351.
Keefe, D. H., Bulen, J. C., Arehart, K. H., and Burns, E. M. (**1993**). "Ear-canal impedance and reflection coefficient in human infants and adults," J. Acoust. Soc. Am. **94**, 2617–2638.
Keefe, D., Hunter, L., Feeney, M., and Fitzpatrick, D. (**2015**). "Procedures for ambient-pressure and tympanometric tests of aural acoustic reflectance and admittance in human infants and adults," J. Acoust. Soc. Am. **138**, 3625–3653.
Møller, A. R. (**2006**). *Hearing: Anatomy, Physiology, and Disorders of the Auditory System*, 2nd ed. (Elsevier, Amsterdam, the Netherlands).
Nørgaard, K. R., Fernandez-Grande, E., and Laugesen, S. (**2017**). "Compensating for evanescent modes and estimating characteristic impedance in waveguide acoustic impedance measurements," J. Acoust. Soc. Am. **142**, 3497–3509.

https://doi.org/10.1121/10.0002358

Pirzanski, C., and Berge, B. (**2002**). "Ear impressions: Art or science?," https://www.audiologyonline.com/articles/ear-impressions-art-or-science-118 (Last viewed August 23, 2020).

Rasetshwane, D. M., and Neely, S. T. (**2011**). "Alternative ear-canal measures related to absorbance," J. Acoust. Soc. Am. **130**, 3873–3881.

R Core Team (**2020**). "R: A Language and Environment for Statistical Computing," R Foundation for Statistical Computing, Vienna, Austria, https://www.R-project.org/ (Last viewed September 15, 2020).

Shahnaz, N., and Bork, K. (**2006**). "Wideband reflectance norms for caucasian and Chinese young adults," Ear Hear. **27**, 774–788.

Souza, N. N., Dhar, S., Neely, S. T., and Siegel, J. H. (**2014**). "Comparison of nine methods to estimate ear-canal stimulus levels," J. Acoust. Soc. Am. **136**, 1768–1787.

Stinson, M. R., and Lawton, B. W. (**1989**). "Specification of the geometry of the human ear canal for the prediction of sound-pressure level distribution," J. Acoust. Soc. Am. **85**, 2492–2503.

Voss, S. E. (**2019**). "Resource review: An online wideband acoustic immittance (wai) database and corresponding website," Ear Hear. **40**, 1481.

Voss, S. E., Horton, N. J., Woodbury, R. R., and Sheffield, K. N. (**2008**). "Sources of variability in reflectance measurements on normal cadaver ears," Ear Hear. **29**, 651–665.

Wever, E. G., and Lawrence, M. (**1954**). *Physiological Acoustics* (Princeton University Press, Princeton, NJ).

Xia, L. (**2017**). "The effects of age, gender, race and ear canal area on normative adult wideband acoustic immittance (wai) measures," Undergraduate thesis, Smith College, Northampton, MA.

Zeger, S. L., and Liang, K.-Y. (**1986**). "Longitudinal data analysis for discrete and continuous outcomes," Biometrics **42**, 121–130.

Zemlin, W. R. (**1988**). *Speech and Hearing Science Anatomy and Physiology*, 3rd ed. (Prentice-Hall, Englewood Cliffs, NJ).